Published in final edited form as:
Exp Neurol. 2010 June ; 223(2): 634–644. doi:10.1016/j.expneurol.2010.02.013.

Chronic intermittent hypoxia reduces neurokinin-1 (NK_1) receptor density in small dendrites of non-catecholaminergic neurons in mouse nucleus tractus solitarius

Andrée Lessard, **Christal G. Coleman**, and **Virginia M. Pickel**
Division of Neurobiology, Department of Neurology and Neuroscience, Weill-Cornell Medical College of Cornell University, New York, NY 10021

Abstract

Chronic intermittent hypoxia (CIH) is a frequent concomitant of sleep apnea, which can increase sympathetic nerve activity through mechanisms involving chemoreceptor inputs to the commissural nucleus of the solitary tract (cNTS). These chemosensory inputs co-store glutamate and substance P (SP), an endogenous ligand for neurokinin-1 (NK_1) receptors. Acute hypoxia results in internalization of NK_1 receptors, suggesting that CIH also may affect the subcellular distribution of NK_1 receptors in subpopulations of cNTS neurons, some of which may express tyrosine hydroxylase, the rate-limiting enzyme for catecholamine synthesis (TH). To test this hypothesis, we examined dual immunolabeling for the NK_1 receptor and TH in the cNTS of male mice subjected to 10 days or 35 days of CIH or intermittent air. Electron microscopy revealed that NK_1 receptors and TH were almost exclusively localized within separate somatodendritic profiles in cNTS of control mice. In dendrites, immunogold particles identifying NK_1 receptors were prevalent in the cytoplasm and on the plasmalemmal surface. Compared with controls, CIH produced a significant region-specific decrease in the cytoplasmic (10 and 35 days, $P< 0.05$, unpaired Student *t*-test) and extrasynaptic plasmalemmal (35 days, $P< 0.01$, unpaired Student *t*-test) density of NK_1 immunogold particles exclusively in small (<0.1 μm) dendrites without TH immunoreactivity. These results suggest that CIH produces a duration-dependent reduction in the availability of NK_1 receptors preferentially in small dendrites of non-catecholaminergic neurons in the cNTS. The implications of our findings are discussed with respect to their potential involvement in the slowly developing hypertension seen in sleep apnea patients.

Keywords

peptide receptors; sleep apnea; hypertension; respiratory reflexes; substance P

Correspondence to Virginia M. Pickel: Division of Neurobiology, Department of Neurology and Neuroscience, Weill Medical College of Cornell University, 407 East 61th Street, room 306, New York, NY 10065, Phone: (646) 962-2900; Fax: (646) 962-0535; vpickel@med.cornell.edu.

Introduction

Chronic intermittent hypoxia (CIH) is an experimental model in which the evoked hypertension reaches levels comparable to those resulting from the sleep-disordered breathing in obstructive sleep apnea (Fletcher, 2001; Xu et al., 2004; Campen et al., 2005; Prabhakar et al., 2007; Smith, 2007). CIH selectively augments the carotid body sensitivity to hypoxia resulting in a long-lasting activation of chemosensory vagal inputs to the medial and commissural nuclei of the solitary tract (cNTS; Prabhakar et al., 2001; Kara et al., 2003). The excitatory transmitters in these sensory vagal inputs include glutamate and substance P (SP; Helke et al., 1980; Douglas et al., 1982; Kalia et al., 1984; Kawano and Chiba, 1984; Kawano and Masuko, 1997; Kawano and Masuko, 1995; Lindefors et al., 1986; Srinivasan et al., 1991), a tachykinin peptide that preferentially acts through G protein coupled neurokinin-1 (NK_1) receptors (Rodier et al., 2001; Rico et al., 2003; Bonham et al., 2004). Moreover, brainstem SP-induced activation of NK_1 receptors can modulate cardiovascular and respiratory responses evoked through the respective baro- and chemoreceptor reflexes (Gillis et al., 1980; Lindefors et al., 1986; Hall et al., 1989; Massari et al., 1998; Zhang et al., 2000; Nattie and Li, 2002). These observations are consistent with the electron microscopic autoradiographic localization of NK_1 receptor binding sites to postsynaptic neurons in the NTS (Jia et al., 1996; Baude and Shigemoto, 1998).

A single hypoxic event increases extracellular concentrations of SP in the NTS (Lindefors et al., 1986; Srinivasan et al., 1991), while decreasing NK_1 receptor binding sites in this region (Mazzone et al., 1997). The SP-activated receptors are internalized into endosomal compartments where they undergo phosphorylation-dependent desensitization and resensitization prior to delivery back to the cell surface (Garland et al., 1996; Grady et al., 1996; Mantyh, 2002). Many NTS neurons co-express NK_1 and glutamate NMDA receptors (Lin et al., 2008), and activation of these NMDA receptors may affect NK_1 receptor trafficking in a manner comparable to that of other G protein coupled receptors (Lin and Huganir, 2007). Thus it is conceivable that CIH-induced enhancement of sympathetic tone is ascribed not only to activity-dependent plasticity of glutamate receptors (de Paula et al., 2007), but also to changes in the availability of NK_1 receptors in cNTS neurons receptive to chemosensory inputs.

Noradrenergic neurons of the A2 group in the intermediate medial and commissural NTS (Kalia et al., 1985) are among those cells receiving visceral vagal inputs (Sumal et al., 1983). The SP activation of NK_1 receptors in these neurons results in a noradrenalin-mediated enhancement of the baroreceptor reflex lowering of blood pressure (Chan et al., 1995). NK_1 receptors have not been previously identified in NTS neurons expressing tyrosine hydroxylase (TH), an enzyme required for synthesis of catecholamines (Le Brun et al., 2008). However, this does not totally exclude the possibility that the acute hypoxia-induced reduction of NK_1 receptor binding sites (Mazzone et al., 1997) and/or the CIH-induced plasticity of these receptors occurs in catecholaminergic and/or non-catecholaminergic neurons of the cNTS. We tested this hypothesis with respect to CIH by quantitatively comparing the electron microscopic immunogold labeling of NK_1 receptors and immunoperoxidase detection of TH in the cNTS of mice exposed to 10 or 35 days of CIH or bursts of room air (the sham controls). A regional comparison was made in the spinal trigeminal nucleus, a nearby brainstem region having an abundance of NK_1 receptors (Li et al., 2000; Aita et al., 2005), and receiving many somatic sensory inputs containing SP (Li et al., 1998a). Our results show that CIH produces a region-specific and duration-dependent decline in the surface expression of NK_1 receptors in small dendrites without TH-immunoreactivity in the cNTS.

Material and Methods

Animal source and care

Male C57BL/6J mice (n=14, Jackson Laboratory, Bar Harbor, ME) of starting weight 22–28g were used for all experiments. These experiments were conducted in accordance with the NIH regulations of animal care and were approved by the Institutional Animal Care and Use Committee of Weill Medical College of Cornell University.

Chronic Intermittent Hypoxia protocol

After two days of acclimation in modified husbandry cages under conditions of 21% oxygen, the mice were randomly separated into CIH and sham controls. In the CIH groups of mice, the home cages were connected to an automated gas delivery system that facilitated rapid transitions from low O_2 levels (10±1%), following nitrogen (N_2) infusion, to ambient concentrations (21±1%), following pure O_2 infusion. Gas (O_2 or N_2) was distributed to the cages over a 5 sec period every 90 sec, resulting in 20 hypoxic episodes per hr. The cycling of O_2 levels occurred for 8 hr during the light (sleep) phase. The control cages were similar in design, but were infused with air every 90 sec to maintain O_2 concentrations at 20–21%. During the remaining 16 hr of the day, both CIH and control cages were infused with room air. The CIH/control protocol repeated for 10 (n= 3 mice/treatment) or 35 (n= 4 mice/treatment) days during which the mice in each treatment group were housed together and had free access to food and water. Ambient temperature was kept at 22–24 °C. This protocol and procedure was developed in our laboratory for group housing mice to minimize intra-animal variability from animal handling and constraints on mobility inherent in the design of other rodent models (Fletcher et al., 1991; Lee et al., 2009; Liu et al., 2009).

At the initiation and termination of the CIH/control protocol, the arterial blood pressure for each mouse was measured using tail-cuff plethysmography (Hatteras Instruments, Cary NC). The pressure level was recorded every two minutes over a 20 min session, and the values were averaged to determine the mean systolic arterial pressure. These values were then combined to obtain the group mean systolic arterial pressure. The tail-cuff is a reliable measure for between group comparisons of mean blood pressure at a given time point, even though this method does not provide absolute measures of mean blood pressure measures when averaged over a 24hr. cycle (Kurtz et al., 2005). An unpaired *t*-test was used to determine whether CIH and control mice had statistically significant ($p<0.05$) differences in systolic blood pressure.

Tissue preparation

On the last experimental day (day 10 or 35), mice were deeply anesthetized by i.p. injection of 100 mg/kg sodium pentobarbital, and then sequentially perfused through the left ventricle of the heart with (1) 5 ml of heparin-saline, (2) 30 ml of 3.75% acrolein in 2% paraformaldehyde, and (3) 75–100 ml of 2% paraformaldehyde in 0.1 M phosphate buffer (PB), pH 7.4. The brains were removed and post-fixed in 2% paraformaldehyde for 30 minutes. Rostrocaudal brain sections (40 μm) were prepared using a Vibratome (Leica Microsystems®, Bannockburn, IL). These sections were then placed in 1% sodium borohydride in PB for 30 minutes to neutralize reactive aldehydes as described in prior studies using acrolein fixation (Leranth and Pickel, 1989). To minimize penetration problems inherent to the pre-embedding methodology, sections used for light and electron microscopy were cryoprotected in 25% sucrose and 3.5% glycerol in PB, rapidly frozen in Freon followed by liquid nitrogen, and thawed in room temperature PB. This rapid freeze-thaw method produces minute holes in the tissue allowing greater penetration of immunoreagents. The sections were then rinsed in 0.1 M Tris-buffered saline (TS). Prior to incubation in primary antisera, the free-floating sections were placed in 0.5% bovine serum albumin (BSA) in 0.1 M TBS for 30 min to block nonspecific

binding of antisera. Sections processed for confocal fluorescence were incubated in a solution of 0.5% BSA in TBS without prior freeze-thaw manipulation.

Antisera

NK_1 receptor localization was achieved by using a well characterized rabbit polyclonal antiserum (Novus Biologicals®, Littleton, CO) against a peptide sequence at the carboxy C-terminus of rat NK_1 receptor (residues 393–407: KTMTESSSFYSNMLA). Light microscopic immunolabeling using the NK_1 receptor antiserum shows a prominent distribution of immunoreactivity along the plasma membrane of rat kidney epithelial cells transfected with a chimeric NK_1 receptor construct, genetically engineered by polymerase chain reaction, while no labeling is seen in cells transfected with the vector alone (Vigna et al., 1994). Light microscopy also revealed an excellent correlation between NK_1 receptor immunoreactivity and ^{125}I-labeled NK_1 receptor-binding sites in the rat central nervous system (Liu et al., 1994). Moreover, binding studies have shown a parallel displacement of ^{125}I-substance P binding to NK_1 receptors by the addition of brain tissue expressing high levels of substance P (Vigna et al., 1994). The localization of the NK_1 receptor antiserum in rat brain is similar to that seen by autoradiographic localization of ^{3}H-substance P (Liu et al., 1994; Mantyh et al., 1995). This antiserum recognizes a protein band of 80–90 kDa on Western blot in brain tissue (Mounir and Parent, 2002). No immunolabeling is seen using this antiserum in sections of brain tissue derived from mice deficient in the NK_1 receptor gene (Lacoste et al., 2006). Similarly, no immunocytochemical labeling is evident in normal brain tissue processed with omission of the NK_1 receptor antiserum or using this antiserum after adsorption with the immunogenic peptide (Liu et al., 1994; Lessard et al., 2009).

The catecholamine phenotype was distinguished by immunolabeling for a mouse monoclonal antibody raised against the full-length tyrosine-hydroxylase (TH) enzyme, which was commercially obtained from Immunostar (Catalog number 22941, Hudson, WI). The TH immunogen was purified to homogeneity from PC12 cells of rat origin. Data provided by Immunostar shows by Western blotting of protein extracts that this monoclonal antibody identifies a 60 kDa immunoreactive band exclusively in TH transfected, but not in non-transfected HEK293 cells. Moreover, in brainstem catecholaminergic cell groups the TH-immunoreactivity seen using this antibody is comparable to the distribution of TH mRNA as seen by *in situ* hybridization (Rusnak and Gainer, 2005). The TH antibody also readily identifies midbrain dopaminergic neurons and brainstem noradrenergic neurons using light or electron microscopic immunolabeling (Pickel et al., 1989; Glass et al., 2001; Lessard and Pickel, 2005; Lane et al., 2008).

Confocal immunofluorescence

Free-floating Vibratome sections were incubated in mouse anti-TH (1:50,000 dilution) and rabbit anti-NK_1 (1:1,000 dilution) antisera for 16 hours at room temperature. Subsequently, the tissue was rinsed several times in TS and then incubated for one hour in a solution containing fluorescein-conjugated (FITC) donkey anti-mouse (TH) and Cy5-conjugated donkey anti-rabbit (Jackson Immunoresearch laboratories Inc., Baltimore, PA) secondary antisera at a dilution of 1:200 in 0.1% BSA in TS. After washes in TS and PB, the tissue sections were mounted in 0.05 M PB onto superfrost glass microslides (VWR International, West Chester, PA). The sections were covered with mounting fluid (Light Diagnostics, Temecula, CA) and glass cover slips, which were sealed along the edges with nail polish to prevent dehydration. These sections were observed on a confocal microscope (Leica TCS SP5; Mannheim, Germany) using sequential laser analysis with emission intensities of 488 nm (Argon, FITC) and 633 nm (Helium, Cy5). Images were produced by LAS AF software (Leica; Mannheim, Germany), imported to *ImageJ* (National Institutes of Health, JAVA 1.60_02) and adjusted for brightness and contrast.

Electron microscopic immunolabeling

Sections used for electron microscopic labeling of TH (immunoperoxidase) and NK_1 receptor (immunogold-silver) were incubated in a primary antisera solution containing mouse anti-TH (1:50,000 dilution) and rabbit anti-NK_1 receptor (1:1,000 dilution) for 24 hours at room temperature, then for 12 hours at 4°C. Following these incubations, the sections were rinsed in TS (0.1 M, pH 7.4) and incubated for 30 min each in biotinylated secondary horse anti-mouse IgG (1:400; Immunostar) and avidin-biotin complex (ABC; Vector, Burlinghame, CA). The tissue was then washed and placed for two hours in a 1:50 dilution of donkey anti-rabbit IgG bound to one nm colloidal gold (Amersham, Arlington, IL) for detection of the rabbit NK_1 receptor antiserum. The gold particles were fixed to the tissue by incubation of the sections in 2% glutaraldehyde in 0.01 M phosphate buffered saline for ten minutes. The particles were enlarged for microscopic examination by reaction in a silver solution from the IntenS-EM kit (GE Healthcare, Piscataway, NJ) for seven minutes at room temperature (Chan et al., 1990). The sections were then postfixed in 2% osmium tetroxide in 0.1 M PB, dehydrated and flat-embedded in epon (19% EM Bed-812; 36% DDSA; 44% NMA; 1% BDMA; Electron Microscopy Sciences, Fort Washington, PA) between two pieces of Aclar plastic (Allied Signal, Pottsville, PA).

An ultramicrotome (Nova, Bromma, Sweden) was used to cut thin sections through the regions of the cNTS and spinal trigeminal nucleus (Sp-5) in coronal Vibratome sections at 8.0 mm posterior to bregma (Franklin and Paxinos, 1997). Subdivisions of the mouse NTS and Sp-5 were determined accordingly to the nomenclature described in the Hof atlas of the mouse brain (Hof et al., 2000). The region of the cNTS extended from the caudal tip of the area postrema to the spinomedullary junction (Baude and Shigemoto, 1998; Colin et al., 2002; Le Brun et al., 2008).

The ultrathin sections through cNTS and Sp-5 were collected on grids and counterstained with Reynold's lead citrate and uranyl acetate (Reynolds, 1963) prior to analysis using a Technai-12 electron microscope (FEI, Heindhoven, The Netherlands). Images were captured using an AMT digital camera, imported to Photoshop software (version 4.0, Adobe Systems, Mountain View, CA), adjusted for sharpness, and then imported to Power Point software (Microsoft Windows ® 2000) for assembly and labeling composite figures.

Electron microscopic data analysis

To assess the distribution of NK_1 receptor immunogold particles, data analysis was performed on ultrathin sections exclusively obtained from the outer (0.1–2 μm) surface of the flat-embedded tissue, where there was optimal penetration of immunoreagents. The profiles containing TH and/or NK_1 immunoreactivity were classified as either neuronal (somata, dendrites, axon terminals) or glial based on criteria from Peters *et. al.* (1991). Peroxidase immunoreactive profiles were recognized by the presence of an electron dense precipitate, whose density and granularity were recognizably distinct from the more homogeneous and lighter density of myelinated axons and other lipidenriched membranes darkened by the osmium tetroxide.

The profiles classified as immunogold-labeled contained two or more gold-silver deposits. The validity of the approach depends on a minimal number of spurious deposits seen on portions of tissue not known to express NK_1 receptors (eg myelin). In our study, myelin rarely showed even one gold particle, representative of non-specific background labeling. In 12,454 μm^2 of cNTS and Sp-5 examined, there were 1383 myelinated axons, of which only 19 had a single NK_1 immunogold particle on the myelin. This suggests the potential of having a 1.4% false-positive labeling with immunogold on identified structures in the size range of myelinated axons. In addition, the labeling in the neuronal cytoplasm was largely restricted to endoplasmic

reticulum and other organelles involved in protein synthesis and/or transport and absent from the nucleus or mitochondria.

At least 50 electron micrographs (magnifications from 13,500X to 34,000X) were obtained from each animal (one or two vibratome sections from each of the mice), in the two regions (cNTS and Sp-5). A total area of 9,762 μm^2 was examined in the cNTS and 2,692 μm^2 in the Sp-5. The profile diameter, area and perimeter were measured by using the Microcomputer Imaging Device software (MCID; Imaging Research, St. Catharines, Ontario, Canada). Parameters used for statistical comparisons were: 1) the number of gold particles on the plasma membrane/perimeter of individual profiles, 2) the number of gold particles in the cytoplasm/cross-sectional area, and 3) the total number (plasmalemmal + non-plasmalemmal) gold particles/profile area. Results are expressed as means ± s.e. mean of (*n*) mice. Results were analyzed for statistical significance by unpaired Student *t*-test (between group comparisons) SPSS for Windows ® Lead Technologies Inc (Chicago, IL). Only probability values (P) less than 0.05 were considered to be statistically significant.

Results

Immunofluorescent microscopic distribution of TH and NK_1 receptors in the cNTS

Confocal microscopic analysis of the cNTS showed immunofluorescence detection of TH in somata and in thick as well as thinner varicose processes that rarely contained NK_1 receptor labeling (Fig. 1A, C). The NK_1 receptors, however, were identified by immunofluorescent product in many non-TH labeled somata and processes within the same region containing TH-immunoreactive neurons (Fig. 1B, C). The neurons expressing majority of the neurons expressing NK_1 receptors were within a medium size range, and usually smaller than those containing TH-immunoreactivity.

Predominant somatodendritic distribution of NK_1 receptors in non-TH containing neurons of cNTS

In sham control and experimental (10 and 35 day CIH) groups of mice, immunogold labeling of NK_1 receptors was confirmed to be almost exclusively located in somatodendritic profiles without detectable TH immunoreactivity when examined by electron microscopy. This is illustrated for control mice (Figs. 2 and 3) in which only 9% (44/490) of all observed NK_1 labeled profiles were TH immunoreactive. After exposure to CIH for either 10 or 35 days, a similarly small percentage (11% in each group) of the NK_1 -labeled profiles in the cNTS contained TH immunoreactivity, and these were exclusively somata and dendrites. In contrast with the abundance of NK_1-labeled dendrites, axon terminals and glial processes rarely contained NK_1 receptor immunogold labeling (Table 1), and none of these co-expressed TH.

Dendritic compartmentation of NK_1 receptors

The NK_1-immunogold particles were mainly located in the cytoplasm near the endoplasmic reticulum and absent from mitochondria in somata (Fig. 2A) and large (> 2 μm diameter) dendrites. These large dendrites were often irregular in contour and difficult to distinguish from portions of somata based on content of organelles and synaptic input. In transverse sections, the remaining dendrites had minimal diameters ranging from 0.2–2.0 μm, and were arbitrarily subdivided into two size-dependent groups; (1) small dendrites measuring 0.2–1.0 μm and medium dendrites measuring 1.1–2.0 μm in minimal diameter. The NK_1-immunogold particles were more commonly aligned along the plasma membrane in the small diameter dendrites (Fig. 2B) in control and in the 10 or 35 day groups of mice (Figs. 3 and 4). The plasmalemmal NK_1-immunogold particles were located along extrasynaptic as well as asymmetric (excitatory-type) or symmetric (inhibitory-type) synaptic portions of the membrane in the cNTS of control and experimental groups of mice (Fig. 4, Table 2).

The density of NK_1 receptor immunogold particles/cross-sectional dendritic area was greater in small dendrites of both control (Fig. 3) and CIH-exposed (Fig 4 and 6) mice. In control mice, the small dendrites contained 66% of the total 1,865 NK_1 immunogold particles, whereas the medium dendrites contained 32%, and large dendrites contained 2% (n= 6/287) of these particles. Similarly, in both the 10 day and 35 day CIH-groups of mice, approximately 60% of the total NK_1 immunogold particles were located in small diameter dendrites.

CIH-induced reduction in NK_1 immunogold in small dendrites of cNTS

The 10 day exposure to CIH produced a qualitative (Fig. 4) and quantitative (Fig. 5) reduction in the cytoplasmic (non-plasmalemmal associated) NK_1 immunogold density in the non-TH containing dendrites. This reduction in cytoplasmic abundance of NK_1 receptor immunogold particles occurred in the small, but not medium diameter dendritic profiles. Because of their infrequent detection, NK_1-labeled large diameter dendrites were not quantitatively analyzed as a separate group.

In contrast with 10 days, 35 days of CIH resulted in a qualitative (Fig. 6) and quantitative (Fig. 7) reduction below control values in both the plasmalemmal and cytoplasmic density of NK_1 immunogold particles in non-TH containing dendrites. These changes were seen only in small dendrites, which have proportionally more NK_1 immunogold particles located on the plasma membrane when compared with medium or large dendrites regardless of experimental conditions. This duration-dependent reduction in plasmalemmal NK_1 receptors in small dendrites of the cNTS paralleled the CIH-induced slow rise in blood pressure, which ranged from 5 to 11 mm Hg at 10 and 35 days, respectively. This blood pressure elevation in the CIH mice also proved to be closer to statistically significant in the 35 day (t-test; p=0.06) compared with the 10 day (t-test; p=0.296) groups.

Regional specificity of NK_1 receptor plasticity in the cNTS compared to spinal trigeminal nucleus

The effects of CIH on NK_1 receptor distribution were region-specific for the cNTS. No significant differences between CIH and control mice were seen in the spinal trigeminal nucleus (Sp-5; Fig. 8). Our observation of prominent NK_1 receptor labeling in Sp-5 is consistent with prior studies (Helke et al., 1984;Nakaya et al., 1994).

Discussion

Our results summarized in Fig. 9 provide the first ultrastructural evidence that CIH produces a selective and significant reduction in intracellular (10 and 35 days) and plasmalemmal (35 days) densities of NK_1 receptors in small dendrites of non-catecholaminergic neurons in the mouse cNTS. The preferential CIH-induced decrease in NK_1 receptor labeling in only the smaller dendrites indicates that CIH may elicit dendritic compartment-specific changes in the functional plasmalemmal and/or synaptic NK_1 receptor expression. The plasmalemmal decrease in NK_1 receptor labeling occurring only at 35 days, a time-point when there is a also greater elevation in arterial pressure than at 10 day, suggests that the surface availability of these receptors may be linked to the long-term detrimental effects of sleep apnea on cardiovascular function.

Methodological considerations

Sleep disturbances are frequent concomitants of CIH in rodents (Hamrahi et al., 2001), but do not appear to contribute significantly to the blood pressure elevation produced by 35 days of CIH (Fletcher et al., 2001). The slightly below statistically significant increase in blood pressure seen after 35 days of CIH in our experiments may reflect the variability in the tail-cuff as a measure of blood pressure, the relatively small number of animals necessitated by

quantitative ultrastructural analysis, and/or the relatively small (11%) magnitude of the blood pressure. Our finding of only a small increase in blood pressure after 35 days of CIH in mice is consistent with many prior studies using comparable hypoxic conditions in rats and/or mice (Fletcher et al., 2001; Campen et al., 2005; Lai et al., 2006). In contrast, however, Peng et al., (2006) found a large (30%) increase in blood pressure after only 10 days of CIH. The greater CIH-induced blood pressure elevation observed by Peng et al., (2006) compared with the present study may result from their use of lower (5% compared with 10%) O_2 levels for generation of the hypoxic episodes.

Somatodendritic NK_1 receptor targeting in non-catecholaminergic neurons

The present location of NK_1 receptors in somatodendritic profiles without TH immunoreactivity in mouse cNTS is consistent with many previous anatomical studies in which few if any NK_1 or NK_3 receptors were identified in A2 and C2 groups of catecholaminergic neurons in rodent NTS (Quirion and Dam, 1986; Saffroy et al., 1988; Mantyh et al., 1989; Jia et al., 1996; Mazzone et al., 1997; Baude and Shigemoto, 1998; Le Brun et al., 2008). The transmitter within these NK_1-containing neurons may include glutamate, since (1) microinjection of SP in the cNTS results in blood pressure elevation (Zhang et al., 2000), and (2) increased blood pressure may result from activation of NTS glutamatergic neurons projecting to sympathoexcitatory neurons in the rostral ventrolateral medulla (RVLM; (Mazzone et al., 1997; Mauad and Machado, 1998; Babic and Ciriello, 2004; Bailey et al., 2004). However, the SP-induced elevation in blood pressure is not blocked by bilateral microinjection of an NK_1 receptor antagonist in the lateral cNTS (Zhang et al., 2000), suggesting a lack of direct involvement of these receptors in mediating chemoreflexes. In contrast, NK_1 receptors in the NTS are highly implicated in bronchopulmonary reflexes that defend the lungs against injury from inhaled agents by the induction of apnea, cough, and hypotension (Mutoh et al., 2000). The latter suggests that at least some of the NK_1 receptors are located in NTS neurons that project not only to the RVLM, but also in those that project to the caudal ventrolateral medulla (CVLM) and decrease sympathetic tone (Kawano and Masuko, 1997). In addition, we cannot exclude the possibility that many of the non-catecholaminergic neurons of the NTS that express NK_1 receptors contain GABA, nitric oxide or other modulators that may indirectly affect sympathetic activity (Stanton et al., 2003; Bailey et al., 2004;).

Size-dependence of CIH-induced changes in dendritic NK_1 receptors

The observed preferential CIH-induced reduction in cytoplasmic (10 day CIH) or cytoplasmic and plasmalemmal (35 day CIH) density of NK_1 receptors in non-TH containing small dendrites of the cNTS may relate to the well established CIH-induced plasticity in the carotid body (Peng et al., 2003; Prabhakar et al., 2005). Chemosensory output neurons in the carotid body contain glutamate and substance P (Srinivasan et al., 1991; Zhang et al., 2000), and often terminate on smaller more distal dendrites of non-catecholaminergic neurons in the commissural and medial NTS (Ruggiero et al., 1994). Our results suggest that the CIH-induced plasticity in the output neurons of the carotid body may in turn affect SP release and NK_1 receptor distribution in their small dendritic targets in the cNTS. In this brain region, the classification of dendrites as small, medium or large is based exclusively on an arbitrary subdivision of all observed NK_1-labeled dendrites into three size-dependent groups as determined from measures of their minimal diameter in transverse sections. These dendrites may include those arising from smaller neurons expressing NK_1 receptors and/or distal portions of dendrites derived from larger neurons that express these receptors.

The CIH-induced reduction in cytoplasmic and plasmalemmal NK_1 receptor density in a selective dendritic compartment suggests that CIH can locally regulate mRNA synthesis and/or degradation, which are known to be primary means for eliciting long-term changes in

synaptic strength (Steward and Schuman, 2001; 2003; Schuman et al., 2006). The hypothesis that CIH may result in decreased production of NK_1 receptors in NTS dendrites is suggested by the fact that a hypoxic stimulus evokes release of SP in this region, and repeated or prolonged exposure to SP produces down regulation of NK_1 receptors in rat, mice and human cells (Organist et al., 1988; Sugiya et al., 1988; Yukhananov and Larson, 1994). Alternatively, CIH may affect degradation and/or rapid recycling to the cell surface induced by acute SP release and/or glutamate, the latter of which is mediated through NMDA receptors (Grady et al., 1995; 1996; Marvizon et al., 1997; Mantyh, 2002) that are often co-expressed with NK_1 receptors in the NTS (Lin et al., 2008).

Regional specificity of CIH-induced reduction in dendritic NK_1 receptors

The effects of CIH on NK_1 receptor density in small dendrites was region-specific for the cNTS and not seen in Sp-5, a brainstem area also expressing many NK_1 receptors (Helke et al., 1984; Mantyh et al., 1984; Covenas et al., 2003). Unlike the cNTS, Sp-5 is mainly involved in relaying nociceptive information to the hypothalamus, the periaqueductal gray matter and thalamus (Li et al., 1996; 1997; 1998b). However, Sp-5 neurons and their NK_1 receptors may also be activated during an acute hypoxic event (LaManna et al., 1996; Mazzone et al., 1997). Although not significant, the small decline in NK_1 receptor density that we observed in the Sp-5 in CIH-exposed mice may indicate a minor role for NK_1 receptors in this region in the adaptive responses to CIH.

Conclusions and implications

We have shown that 10 days of CIH is sufficient to reduce the cytoplasmic density of NK_1 receptor immunolabeling in small dendrites of non-catecholaminergic neurons in the cNTS. However, 35 days of CIH is effective in depletion of the cytoplasmic as well as extrasynaptic and plasmalemmal NK_1 receptors in these dendrites. This more prominent 35 day CIH-induced depletion of surface NK_1 receptors in small dendrites of the cNTS occurred concomitantly with a strong trend toward increase blood pressure that is consistent with the established chemosensory-dependent hypertension reported in CIH rodent models (Prabhakar et al., 2001) and in sleep apnea patients (Smith and Pacchia, 2007).

Acknowledgments

This research was supported by NIH grants (HL18974 and HL096571)

Literature Cited

Aita M, Seo K, Fujiwara N, Takagi R, Maeda T. Postnatal changes in the spatial distributions of substance P and neurokinin-1 receptor in the trigeminal subnucleus caudalis of mice. Brain Res Dev Brain Res 2005;155:33–41.

Babic T, Ciriello J. Medullary and spinal cord projections from cardiovascular responsive sites in the rostral ventromedial medulla. J Comp Neurol 2004;469:391–412. [PubMed: 14730590]

Bailey CP, Maubach KA, Jones RS. Neurokinin-1 receptors in the rat nucleus tractus solitarius: pre- and postsynaptic modulation of glutamate and GABA release. Neuroscience 2004;127:467–479. [PubMed: 15262336]

Baude A, Shigemoto R. Cellular and subcellular distribution of substance P receptor immunoreactivity in the dorsal vagal complex of the rat and cat: a light and electron microscope study. J Comp Neurol 1998;402:181–196. [PubMed: 9845242]

Bonham AC, Sekizawa SI, Joad JP. Plasticity of central mechanisms for cough. Pulm Pharmacol Ther 2004;17:453–457. [PubMed: 15564091]

Campen MJ, Shimoda LA, O'Donnell CP. Acute and chronic cardiovascular effects of intermittent hypoxia in C57BL/6J mice. J Appl Physiol 2005;99:2028–2035. [PubMed: 16002771]

Chan J, Aoki C, Pickel VM. Optimization of differential immunogold-silver and peroxidase labeling with maintenance of ultrastructure in brain sections before plastic embedding. J Neurosci Methods 1990;33:113–127. [PubMed: 1977960]

Chan JYH, Tsou M-Y, Len W-B, Lee T-Y, Chan SHH. Participation of noradrenergic neurotransmission in the enhancement of baroreceptor reflex response by substance P at the nucleus tractus solitarii of the rat: A reverse microdialysis study. J Neurochem 1995;64:2644–2652. [PubMed: 7539056]

Colin I, Blondeau C, Baude A. Neurokinin release in the rat nucleus of the solitary tract via NMDA and AMPA receptors. Neuroscience 2002;115:1023–1033. [PubMed: 12453476]

Covenas R, Martin F, Belda M, Smith V, Salinas P, Rivada E, Diaz-Cabiale Z, Narvaez JA, Marcos P, Tramu G, Gonzalez-Baron S. Mapping of neurokinin-like immunoreactivity in the human brainstem. BMC Neurosci 2003;4:3. [PubMed: 12617753]

de Paula PM, Tolstykh G, Mifflin SW. Chronic intermittent hypoxia alters NMDA and AMPA-evoked currents in NTS neurons receiving carotid body chemoreceptor inputs. Am J Physiol Regul Integr Comp Physiol. 2007

Douglas FL, Palkovits M, Brownstein MJ. Regional distribution of substance P-like immunoreactivity in the lower brainstem of the rat. Brain Res 1982;245:376–378. [PubMed: 6181848]

Fletcher EC. Invited review: Physiological consequences of intermittent hypoxia: systemic blood pressure. J Appl Physiol 2001;90:1600–1605. [PubMed: 11247966]

Franklin, KBJ.; Paxinos, G. The mouse brain in stereotaxic coordinates. San Diego: Academic Press; 1997.

Garland AM, Grady EF, Lovett M, Vigna SR, Frucht MM, Krause JE, Bunnett NW. Mechanisms of desensitization and resensitization of G protein-coupled neurokinin1 and neurokinin2 receptors. Mol Pharmacol 1996;49:438–446. [PubMed: 8643083]

Gillis RA, Helke CJ, Hamilton BL, Norman WP, Jacobowitz DM. Evidence that substance P is a neurotransmitter of baro- and chemoreceptor afferents in nucleus tractus solitarius. Brain Res 1980;181:476–481. [PubMed: 6243228]

Glass MJ, Huang J, Aicher SA, Milner TA, Pickel VM. Subcellular localization of alpha-2A-adrenergic receptors in the rat medial nucleus tractus solitarius: regional targeting and relationship with catecholamine neurons. J Comp Neurol 2001;433:193–207. [PubMed: 11283959]

Grady EF, Gamp PD, Jones E, Baluk P, McDonald DM, Payan DG, Bunnett NW. Endocytosis and recycling of neurokinin 1 receptors in enteric neurons. Neuroscience 1996;75:1239–1254. [PubMed: 8938757]

Grady EF, Garland AM, Gamp PD, Lovett M, Payan DG, Bunnett NW. Delineation of the endocytic pathway of substance P and its seven-transmembrane domain NK1 receptor. Mol Biol Cell 1995;6:509–524. [PubMed: 7545030]

Hall ME, Miley FB, Stewart JM. Cardiovascular effects of substance P peptides in the nucleus of the solitary tract. Brain Res 1989;497:280–290. [PubMed: 2479449]

Hamrahi H, Stephenson R, Mahamed S, Liao KS, Horner RL. Selected Contribution: Regulation of sleep-wake states in response to intermittent hypoxic stimuli applied only in sleep. J Appl Physiol 2001;90:2490–2501. [PubMed: 11356818]

Helke CJ, O'Donohue TL, Jacobowitz DM. Substance P as a baro- and chemoreceptor afferent neurotransmitter: immunocytochemical and neurochemical evidence in the rat. Peptides 1980;1:1–9. [PubMed: 6165975]

Helke CJ, Shults CW, Chase TN, ODonohue TL. Autoradiographic localization of substance P receptors in rat medulla: effect of vagotomy and nodose ganglionectomy. Neurosci 1984;12:215–223.

Hof PR, Young WG, Bloom FE, Belichenko PV, Celio MR. Comparative cytoarchitectonic atlas of the C57BL/6 and 129/SV mouse brains. Elsevier. 2000

Jia HG, Wang BR, Rao ZR, Shi JW, Shigemoto R, Kaneko T, Mizuno N. GABAergic synapses upon neurons expressing substance P receptors in the nucleus of the solitary tract: an immunocytochemical electron microscope study in the rat. Neurosci Lett 1996;210:49–52. [PubMed: 8762189]

Kalia M, Fuxe K, Goldstein M. Rat medulla oblongata. II. Dopaminergic, noradrenergic (A1 and A2) and adrenergic neurons, nerve fibers, and presumptive terminal processes. J Comp Neurol 1985;233:308–332. [PubMed: 2858497]

Kalia M, Fuxe K, Hokfelt T, Johansson O, Lang R, Ganten D, Cuello C, Terenius L. Distribution of neuropeptide immunoreactive nerve terminals within the subnuclei of the nucleus of the tractus solitarius of the rat. J Comp Neurol 1984;222:409–444. [PubMed: 6199382]

Kara T, Narkiewicz K, Somers VK. Chemoreflexes--physiology and clinical implications. Acta Physiol Scand 2003;177:377–384. [PubMed: 12609009]

Kawano H, Chiba T. Distribution of substance P immunoreactive nerve terminals within the nucleus tractus solitarius of the rat. Neurosci Lett 1984;45:175–179. [PubMed: 6203063]

Kawano H, Masuko S. Substance P innervation of neurons projecting to the paraventricular hypothalamic nucleus in the rat nucleus tractus solitarius. Brain Res 1995;689:136–140. [PubMed: 8528697]

Kawano H, Masuko S. Synaptic contacts of substance P-immunoreactive axon terminals in the nucleus tractus solitarius onto neurons projecting to the caudal ventrolateral medulla oblongata in the rat. Brain Res 1997;754:315–320. [PubMed: 9134991]

Kurtz TW, Griffin KA, Bidani AK, Davisson RL, Hall JE. Recommendations for blood pressure measurement in humans and experimental animals. Part 2: Blood pressure measurement in experimental animals: a statement for professionals from the subcommittee of professional and public education of the American Heart Association council on high blood pressure research. Hypertension 2005;45:299–310. [PubMed: 15611363]

Lacoste B, Riad M, Descarries L. Immunocytochemical evidence for the existence of substance P receptor (NK1) in serotonin neurons of rat and mouse dorsal raphe nucleus. Eur J Neurosci 2006;23:2947–2958. [PubMed: 16819984]

Lai CJ, Yang CC, Hsu YY, Lin YN, Kuo TB. Enhanced sympathetic outflow and decreased baroreflex sensitivity are associated with intermittent hypoxia-induced systemic hypertension in conscious rats. J Appl Physiol 2006;100:1974–1982. [PubMed: 16484362]

LaManna JC, Haxhiu MA, Kutina-Nelson KL, Pundik S, Erokwu B, Yeh ER, Lust WD, Cherniack NS. Decreased energy metabolism in brain stem during central respiratory depression in response to hypoxia. J Appl Physiol 1996;81:1772–1777. [PubMed: 8904598]

Lane DA, Lessard AA, Chan J, Colago EE, Zhou Y, Schlussman SD, Kreek MJ, Pickel VM. Region-specific changes in the subcellular distribution of AMPA receptor GluR1 subunit in the rat ventral tegmental area after acute or chronic morphine administration. J Neurosci 2008;28:9670–9681. [PubMed: 18815253]

Le Brun I, Dufour A, Crest M, Szabo G, Erdelyi F, Baude A. Differential expression of Nk1 and NK3 neurokinin receptors in neurons of the nucleus tractus solitarius and the dorsal vagal motor nucleus of the rat and mouse. Neuroscience 2008;152:56–64. [PubMed: 18222044]

Lee EJ, Woodske ME, Zou B, O'Donnell CP. Dynamic arterial blood gas analysis in conscious, unrestrained C57BL/6J mice during exposure to intermittent hypoxia. J Appl Physiol 2009;107:290–294. [PubMed: 19056995]

Leranth, C.; Pickel, VM. Electron microscopic pre-embedding double immunostaining methods. In: Heimer, L.; Zaborszky, L., editors. Neuroanatomical Tract-tracing Methods 2: Recent Progress. New York: Plenum Publishing Co.; 1989. p. 129-172.

Lessard A, Pickel VM. Subcellular distribution and plasticity of neurokinin-1 receptors in the rat substantia nigra and ventral tegmental area. Neuroscience 2005;135:1309–1323. [PubMed: 16165296]

Lessard A, Savard M, Gobeil F Jr, Pierce JP, Pickel VM. The neurokinin-3 (NK(3) and the neurokinin-1 (NK(1) receptors are differentially targeted to mesocortical and mesolimbic projection neurons and to neuronal nuclei in the rat ventral tegmental area. Synapse 2009;63(6):484–501. [PubMed: 19224600]

Li JL, Ding YQ, Li YQ, Li JS, Nomura S, Kaneko T, Mizuno N. Immunocytochemical localization of mu-opioid receptor in primary afferent neurons containing substance P or calcitonin gene-related peptide. A light and electron microscope study in the rat. Brain Res 1998a;794:347–352. [PubMed: 9622672]

Li JL, Ding YQ, Shigemoto R, Mizuno N. Distribution of trigeminothalamic and spinothalamic-tract neurons showing substance P receptor-like immunoreactivity in the rat. Brain Res 1996;719:207–212. [PubMed: 8782883]

Li JL, Ding YQ, Xiong KH, Li JS, Shigemoto R, Mizuno N. Substance P receptor (NK1)-immunoreactive neurons projecting to the periaqueductal gray: distribution in the spinal trigeminal nucleus and the spinal cord of the rat. Neurosci Res 1998b;30:219–225. [PubMed: 9593332]

Li JL, Kaneko T, Shigemoto R, Mizuno N. Distribution of trigeminohypothalamic and spinohypothalamic tract neurons displaying substance P receptor-like immunoreactivity in the rat. J Comp Neurol 1997;378:508–521. [PubMed: 9034907]

Li JL, Wang D, Kaneko T, Shigemoto R, Nomura S, Mizuno N. The relationship between neurokinin-l receptor and substance P in the medullary dorsal horn - A light and electron microscopic immunohistochemical study in the rat. Neuroscience Research 2000;36:327–334. [PubMed: 10771111]

Lin DT, Huganir RL. PICK1 and Phosphorylation of the Glutamate Receptor 2 (GluR2) AMPA Receptor Subunit Regulates GluR2 Recycling after NMDA Receptor-Induced Internalization. J Neurosci 2007;27:13903–13908. [PubMed: 18077702]

Lin LH, Taktakishvili OM, Talman WT. Colocalization of neurokinin-1, N-methyl-D-aspartate, and AMPA receptors on neurons of the rat nucleus tractus solitarii. Neuroscience 2008;154:690–700. [PubMed: 18479828]

Lindefors N, Yamamoto Y, Pantaleo T, Lagercrantz H, Brodin E, Ungerstedt U. In vivo release of substance P in the nucleus tractus solitarii increases during hypoxia. Neurosci Lett 1986;69:94–97. [PubMed: 2427979]

Liu H, Brown JL, Jasmin L, Maggio JE, Vigna SR, Mantyh PW, Basbaum AI. Synaptic relationship between substance P and the substance P receptor: light and electron microscopic characterization of the mismatch between neuropeptides and their receptors. Proc Natl Acad Sci U S A 1994;91:1009–1013. [PubMed: 7508118]

Liu Y, Ji ES, Xiang S, Tamisier R, Tong J, Huang J, Weiss JW. Exposure to cyclic intermittent hypoxia increases expression of functional NMDA receptors in the rat carotid body. J Appl Physiol 2009;106:259–267. [PubMed: 18927268]

Mantyh PW. Neurobiology of substance P and the NK1 receptor. J Clin Psychiatry 2002;63:6–10. [PubMed: 12562137]

Mantyh PW, Allen CJ, Ghilardi JR, Rogers SD, Mantyh CR, Liu H, Basbaum AI, Vigna SR, Maggio JE. Rapid endocytosis of a G protein-coupled receptor: substance P evoked internalization of its receptor in the rat striatum in vivo. Proc Natl Acad Sci U S A 1995;92:2622–2626. [PubMed: 7535928]

Mantyh PW, Gates T, Mantyh CR, Maggio JE. Autoradiographic localization and characterization of tachykinin receptor binding sites in the rat brain and peripheral tissues. J Neurosci 1989;9:258–279. [PubMed: 2536418]

Mantyh PW, Hunt SP, Maggio JE. Substance P receptors: localization by light microscopic autoradiography in rat brain using [3H]SP as the radioligand. Brain Res 1984;307:147–165. [PubMed: 6087984]

Marvizon JC, Martinez V, Grady EF, Bunnett NW, Mayer EA. Neurokinin 1 receptor internalization in spinal cord slices induced by dorsal root stimulation is mediated by NMDA receptors. J Neurosci 1997;17:8129–8136. [PubMed: 9334388]

Massari VJ, Shirahata M, Johnson TA, Lauenstein JM, Gatti PJ. Substance P immunoreactive nerve terminals in the dorsolateral nucleus of the tractus solitarius: Roles in the baroreceptor reflex. Brain Res 1998;785:329–340. [PubMed: 9518676]

Mauad H, Machado BH. Involvement of the ipsilateral rostral ventrolateral medulla in the pressor response to L-glutamate microinjection into the nucleus tractus solitarii of awake rats. Journal of the Autonomic Nervous System 1998;74:43–48. [PubMed: 9858123]

Mazzone SB, Hinrichsen CF, Geraghty DP. Substance P receptors in brain stem respiratory centers of the rat: regulation of NK1 receptors by hypoxia. J Pharmacol Exp Ther 1997;282:1547–1556. [PubMed: 9316871]

Mounir S, Parent A. The expression of neurokinin-1 receptor at striatal and pallidal levels in normal human brain. Neurosci Res 2002;44:71–81. [PubMed: 12204295]

Mutoh T, Bonham AC, Joad JP. Substance P in the nucleus of the solitary tract augments bronchopulmonary C fiber reflex output. Am J Physiol Regul Integr Comp Physiol 2000;279:R1215–R1223. [PubMed: 11003986]

Nakaya Y, Kaneko T, Shigemoto R, Nakanishi S, Mizuno N. Immunohistochemical localization of substance P receptor in the central nervous system of the adult rat. J Comp Neurol 1994;347:249–274. [PubMed: 7814667]

Nattie EE, Li A. Substance P-saporin lesion of neurons with NK1 receptors in one chemoreceptor site in rats decreases ventilation and chemosensitivity. J Physiol 2002;544:603–616. [PubMed: 12381830]

Organist ML, Harvey JP, McGillis JP, Payan DG. Processing of the human IM-9 lymphoblast substance P receptor. Biosynthetic and degradation studies using a monoclonal anti-receptor antibody. Biochem Biophys Res Commun 1988;151:535–541. [PubMed: 2450542]

Peng YJ, Overholt JL, Kline D, Kumar GK, Prabhakar NR. Induction of sensory long-term facilitation in the carotid body by intermittent hypoxia: implications for recurrent apneas. Proc Natl Acad Sci U S A 2003;100:10073–10078. [PubMed: 12907705]

Peng YJ, Yuan G, Ramakrishnan D, Sharma SD, Bosch-Marce M, Kumar GK, Semenza GL, Prabhakar NR. Heterozygous HIF-1alpha deficiency impairs carotid body-mediated systemic responses and reactive oxygen species generation in mice exposed to intermittent hypoxia. J Physiol 2006;577:705–716. [PubMed: 16973705]

Peters, A.; Palay, SL.; Webster, Hd. The Fine Structure of the Nervous System. New York: Oxford University Press; 1991.

Pickel VM, Chan J, Milner TA. Ultrastructural basis for interactions between central opioids and catecholamines. II. Nuclei of the solitary tracts. J Neurosci 1989;9:2519–2535. [PubMed: 2568412]

Prabhakar NR, Dick TE, Nanduri J, Kumar GK. Systemic, cellular and molecular analysis of chemoreflex-mediated sympathoexcitation by chronic intermittent hypoxia. Exp Physiol 2007;92:39–44. [PubMed: 17124274]

Prabhakar NR, Fields RD, Baker T, Fletcher EC. Intermittent hypoxia: cell to system. Am J Physiol Lung Cell Mol Physiol 2001;281:L524–L528. [PubMed: 11504675]

Prabhakar NR, Peng YJ, Jacono FJ, Kumar GK, Dick TE. Cardiovascular alterations by chronic intermittent hypoxia: importance of carotid body chemoreflexes. Clin Exp Pharmacol Physiol 2005;32:447–449. [PubMed: 15854156]

Quirion R, Dam TV. Ontogeny of substance P receptor binding sites in rat brain. J Neurosci 1986;6:2187–2199. [PubMed: 3018188]

Reynolds ES. The use of lead citrate at high pH as an electron-opaque stain in electron microscopy. J Cell Biol 1963;17:208. [PubMed: 13986422]

Rico AJ, Prieto-Lloret J, Donnelly DF, De FC, Gonzalez C, Rigual R. The use of NK-1 receptor null mice to assess the significance of substance P in the carotid body function. Adv Exp Med Biol 2003;536:327–336. [PubMed: 14635685]

Rodier ME, Laferriere A, Moss IR. Effects of age and clustered hypoxia on [(125)I] substance P binding to neurotachykinin-1 receptors in brainstem of developing swine. Brain Res Dev Brain Res 2001;127:31–39.

Ruggiero, DA.; Pickel, VM.; Milner, TA.; Anwar, M.; Otake, K.; Mtui, EP.; Park, D. Viscerosensory processing in nucleus tractus solitarii: structural and neurochemical substrates. In: Barraco, IRA., editor. Nucleus of the Solitary Tract. Boca Raton: CRC Press; 1994. p. 3-34.

Rusnak M, Gainer H. Differential effects of forskolin on tyrosine hydroxylase gene transcription in identified brainstem catecholaminergic neuronal subtypes in organotypic culture. Eur J Neurosci 2005;21:889–898. [PubMed: 15787695]

Saffroy M, Beaujouan JC, Torrens Y, Besseyre J, Bergstrom L, Glowinski J. Localization of tachykinin binding sites (NK1, NK2, NK3 ligands) in the rat brain. Peptides 1988;9:227–241. [PubMed: 2836823]

Schuman EM, Dynes JL, Steward O. Synaptic regulation of translation of dendritic mRNAs. J Neurosci 2006;26:7143–7146. [PubMed: 16822969]

Smith ML. Sleep apnoea and hypertension: physiological bases for a causal relation themed issue. Exp Physiol 2007;92:19–20. [PubMed: 17259300]

Smith ML, Pacchia CF. Sleep apnoea and hypertension: role of chemoreflexes in humans. Exp Physiol 2007;92:45–50. [PubMed: 17099063]

Srinivasan M, Goiny M, Pantaleo T, Lagercrantz H, Brodin E, Runold M, Yamamoto Y. Enhanced in vivo release of substance P in the nucleus tractus solitarii during hypoxia in the rabbit: role of peripheral input. Brain Res 1991;546:211–216. [PubMed: 1712658]

Stanton PK, Winterer J, Bailey CP, Kyrozis A, Raginov I, Laube G, Veh RW, Nguyen CQ, Muller W. Long-term depression of presynaptic release from the readily releasable vesicle pool induced by NMDA receptor-dependent retrograde nitric oxide. J Neurosci 2003;23:5936–5944. [PubMed: 12843298]

Steward O, Schuman EM. Protein synthesis at synaptic sites on dendrites. Annu Rev Neurosci 2001;24:299–325. [PubMed: 11283313]

Steward O, Schuman EM. Compartmentalized synthesis and degradation of proteins in neurons. Neuron 2003;40:347–359. [PubMed: 14556713]

Sugiya H, Obie JF, Putney JW Jr. Two modes of regulation of the phospholipase C-linked substance-P receptor in rat parotid acinar cells. Biochem J 1988;253:459–466. [PubMed: 2460079]

Sumal KK, Blessing WW, Joh TH, Reis DJ, Pickel VM. Synaptic interaction of vagal afferents and catecholaminergic neurons in the rat nucleus tractus solitarius. Brain Res 1983;277:31–40. [PubMed: 6139145]

Vigna SR, Bowden JJ, McDonald DM, Fisher J, Okamoto A, McVey DC, Payan DG, Bunnett NW. Characterization of antibodies to the rat substance P (NK- 1) receptor and to a chimeric substance P receptor expressed in mammalian cells. J Neurosci 1994;14:834–845. [PubMed: 7507985]

Xu W, Chi L, Row BW, Xu R, Ke Y, Xu B, Luo C, Kheirandish L, Gozal D, Liu R. Increased oxidative stress is associated with chronic intermittent hypoxia-mediated brain cortical neuronal cell apoptosis in a mouse model of sleep apnea. Neuroscience 2004;126:313–323. [PubMed: 15207349]

Yukhananov RY, Larson AA. An N-terminal fragment of substance P, substance P(1–7), down-regulates neurokinin-1 binding in the mouse spinal cord. Neurosci Lett 1994;178:163–166. [PubMed: 7529387]

Zhang C, Bonagamba LG, Machado BH. Blockade of NK-1 receptors in the lateral commissural nucleus tractus solitarii of awake rats had no effect on the cardiovascular responses to chemoreflex activation. Braz J Med Biol Res 2000;33:1379–1385. [PubMed: 11050671]

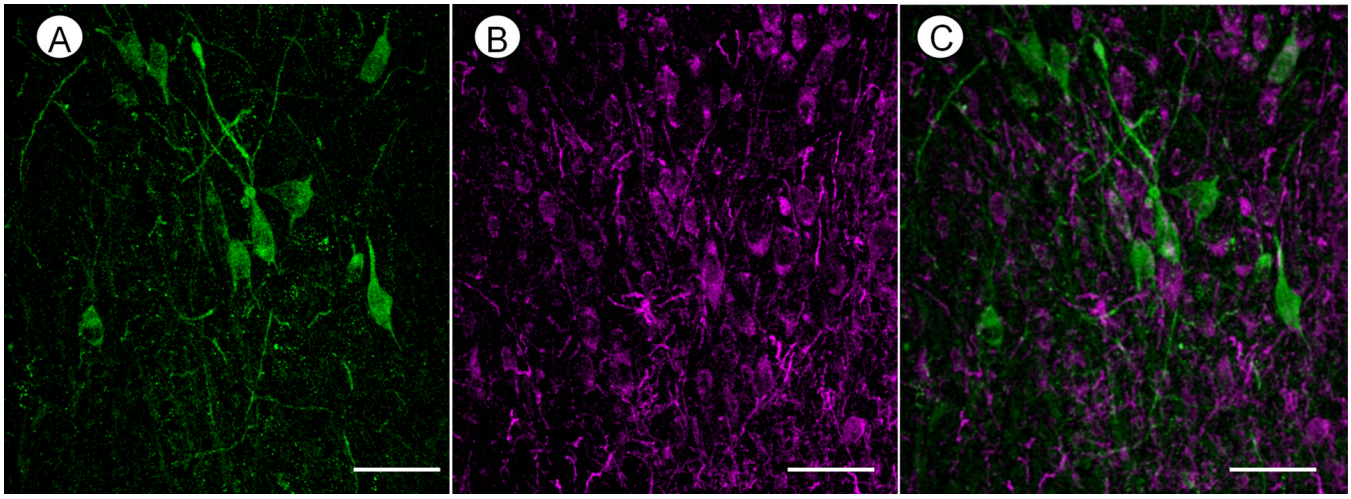

Fig. 1.

Confocal micrographs showing immunofluorescence labeling for TH (green, A) and NK_1 receptor (purple, B) in somata and processes in cNTS of a control mouse. The merged image (C) reveals that NK_1-labeled profiles are mainly without TH immunoreactivity. Scale bars: 50 μm.

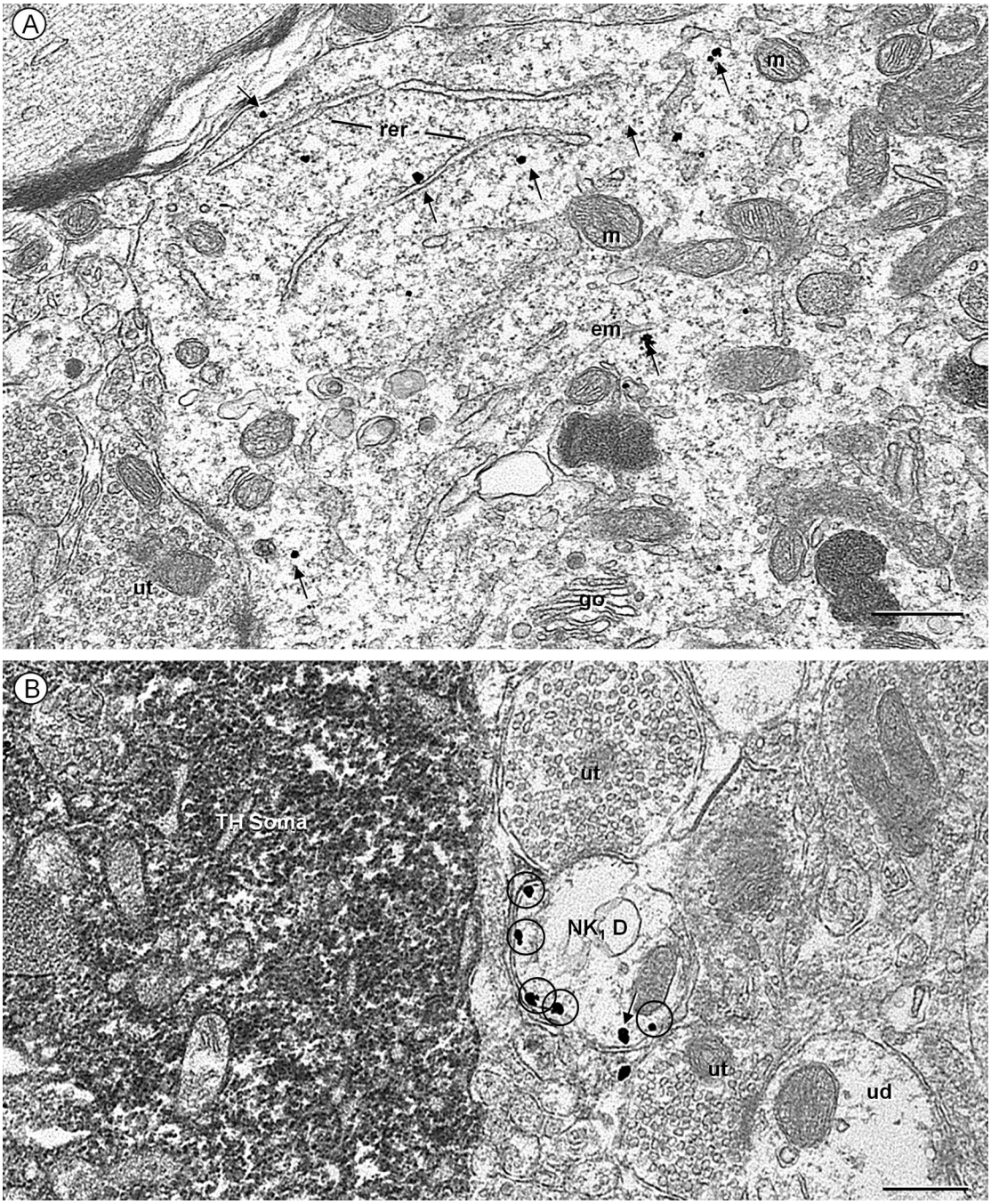

Fig. 2.

Electron micrographs displaying NK_1 receptor (immunogold) in a soma (A) and dendrite (B) located within the cNTS of a control mouse. These structures are without detectable tyrosine hydroxylase (TH, immunoperoxidase) immunoreactivity, such as that seen in a nearby soma (TH-soma of B). A. NK_1 immunogold particles (arrows) are seen throughout the cytosol in a soma receiving input from an unlabeled terminal (ut). The labeling is particularly evident near the rough endoplasmic reticulum (rer), Golgi apparatus (go) and endomembranes (em), but absent from mitochondria (m). B. Many extrasynaptic plasmalemmal NK_1 immunogold particles (encircled) are seen in a transversely sectioned NK_1-labeled dendrite (NK_1 D). This

dendrite is located in a neuropil that contains a TH-labeled soma as well as unlabeled terminals (ut) and dendrites (ud). Scale bar: 0.5 μm.

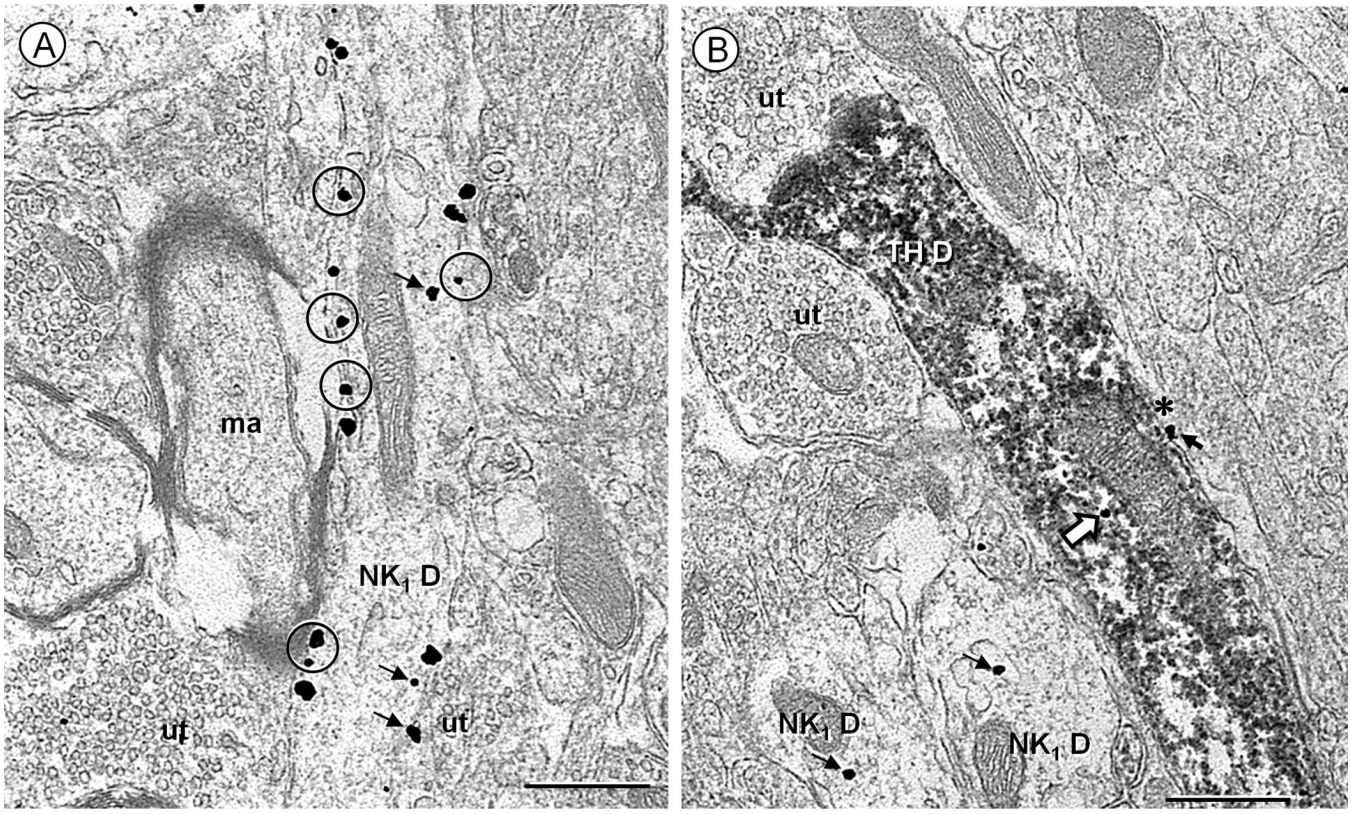

Fig. 3.

Electron micrographs showing the ultrastructural localization of NK_1 receptor (immunogold) and tyrosine hydroxylase (TH, immunoperoxidase) immunoreactivity in the cNTS of a control mouse. A. Many NK_1 immunogold particles are aligned along the plasma membrane (circles), or in the cytoplasm (small arrows) distant from the surface in a longitudinally sectioned dendrite (NK_1 D). The dendrite is opposed by unlabeled terminals (ut) and a myelinated axon (ma). B. An isolated NK_1 immunogold particle (block arrow) is located in the cytoplasm of a longitudinally sectioned dendrite showing diffuse peroxidase reaction product for TH (TH-D) and contacted by unlabeled axon terminals (ut). Other NK_1 immunogold particles (small arrows) are seen in two nearby transversely sectioned dendrites (NK_1 D) and in a glial process (asterisk) opposing the TH-immunoreactive dendrite. Scale bar: 0.5 μm.

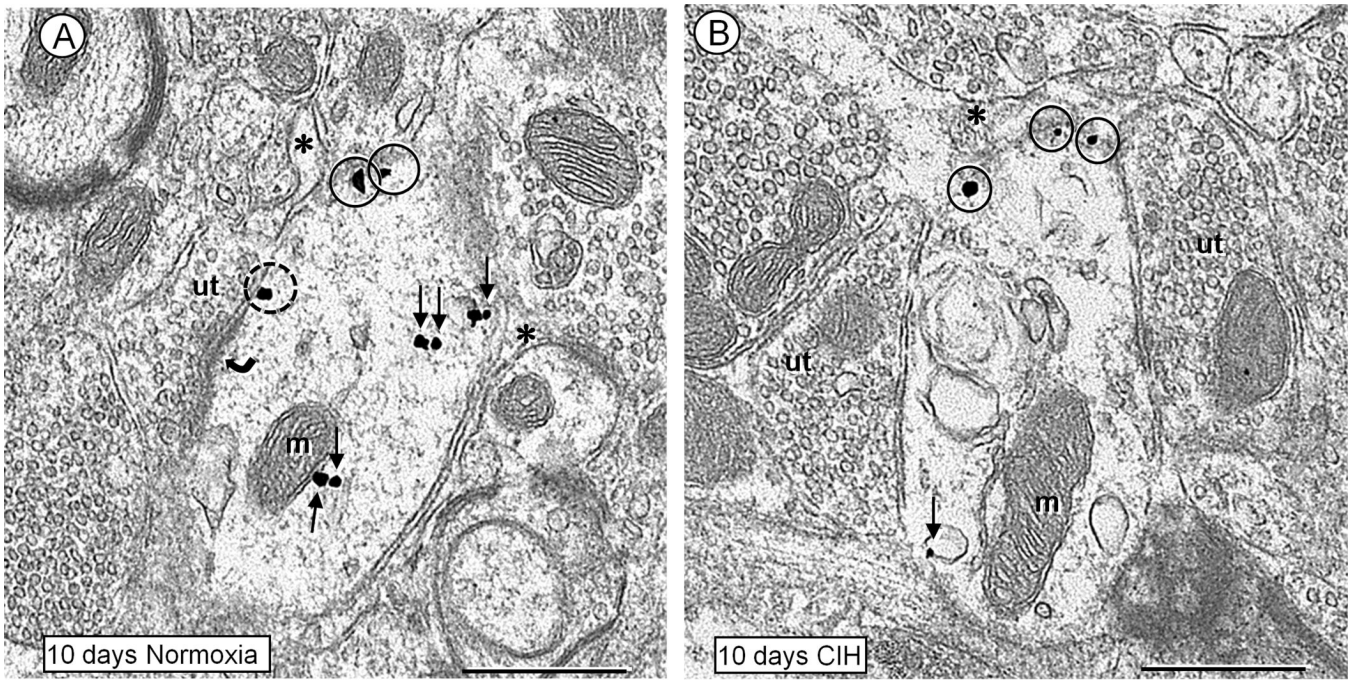

Fig. 4.

Electron micrographs showing the plasmalemmal and cytoplasmic distributions of NK_1 receptor immunogold particles in non-TH containing dendrites within the cNTS of mice receiving bursts of room air (A) or CIH (B) for 10 days. A. Coronal section of a dendrite in control condition, where NK_1 immunogold particles are seen in the cytosol (small arrows), and along the extrasynaptic (closed circles) or perisynaptic (dashed circle) plasma membranes near an asymmetric synapse (curved arrow) from an unlabeled terminal (ut). The dendrite is also contacted by a thin glial process (asterisks). B. Coronal section of a transversely sectioned dendrite in the cNTS of mouse exposed to 10 days of CIH. As compared to the control in A, there is a notable reduction in the cytoplasmic (small arrow), but not extrasynaptic plasmalemmal (closed circles) NK_1 immunogold particles in this dendrite. The labeled dendrite is contacted by a glial process (asterisk) and two unlabeled axon terminals (ut) showing poorly defined synapses that appear to have symmetric membrane specializations. Scale bars: 0.5 μm.

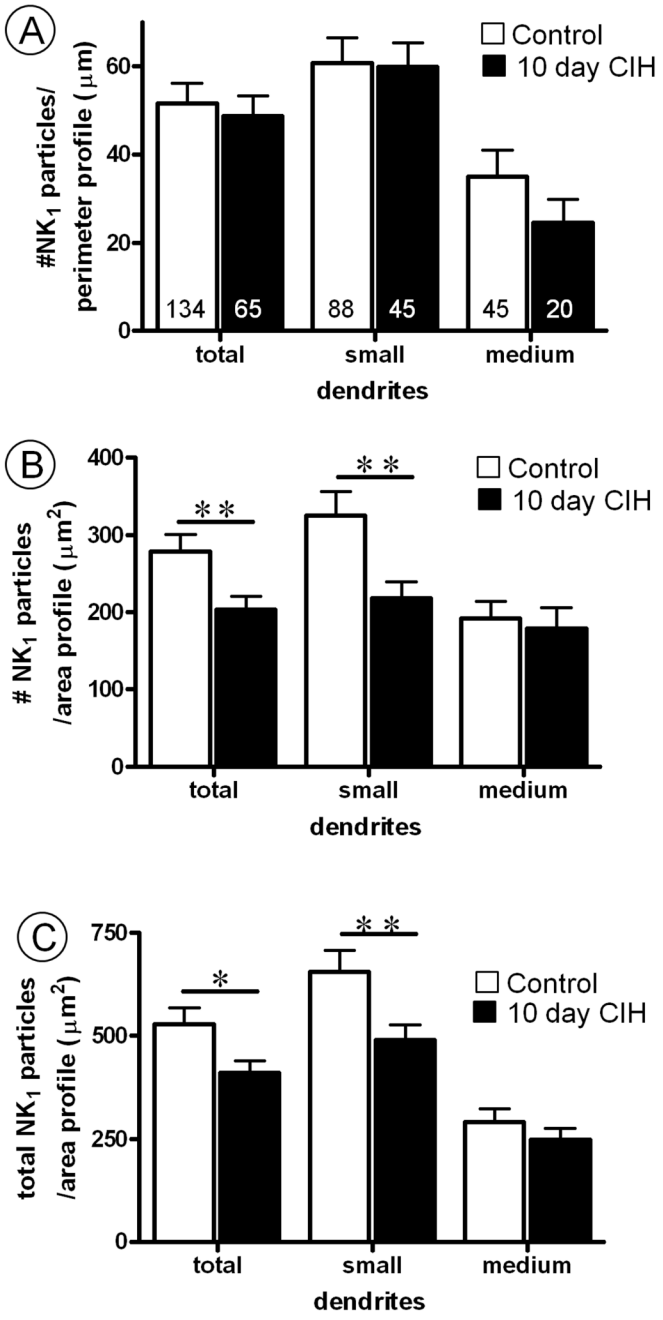

Fig. 5.

Bar graphs showing (A) plasmalemmal, (B) cytoplasmic and (C) total (plasmalemmal and cytoplasmic) NK_1 receptor density in non-TH containing dendrites of the cNTS of control mice, as compared to mice subjected to 10 days of chronic intermittent hypoxia (CIH). In A, the values are shown as ratio of the number of NK_1-immunogold particles contacting the dendritic plasma membrane/perimeter length (100 μm). Numbers in bars represent the number of transversely sectioned dendritic profiles. In B, the ratios indicate as the number of cytoplasmic NK_1 immunogold particles located at a distance from the plasma membrane/area of dendritic profiles (100 μm^2). In C, the ratios represent the total number of NK_1 immunogold particles/area of the dendritic profile (100 μm^2). Vertical bars represent the mean ± S.E. mean

of (n) dendrites in each group. Statistical comparisons were made between control and 10 day CIH mice in groups including all transversely cut non-TH containing dendritic profiles (total) or in subgroups of these dendritic profiles separated into small (<1 μm, 66–68% of total dendrites) and medium (1–2 μm, 31–33% of total dendrites) categories according to their minimal cross-sectional diameter. Data were obtained from six vibratome sections, one for each of the three control and three ten day CIH mice analyzed. Significant differences were determined using an unpaired Student *t*-test. **P< 0.01, *P< 0.05.

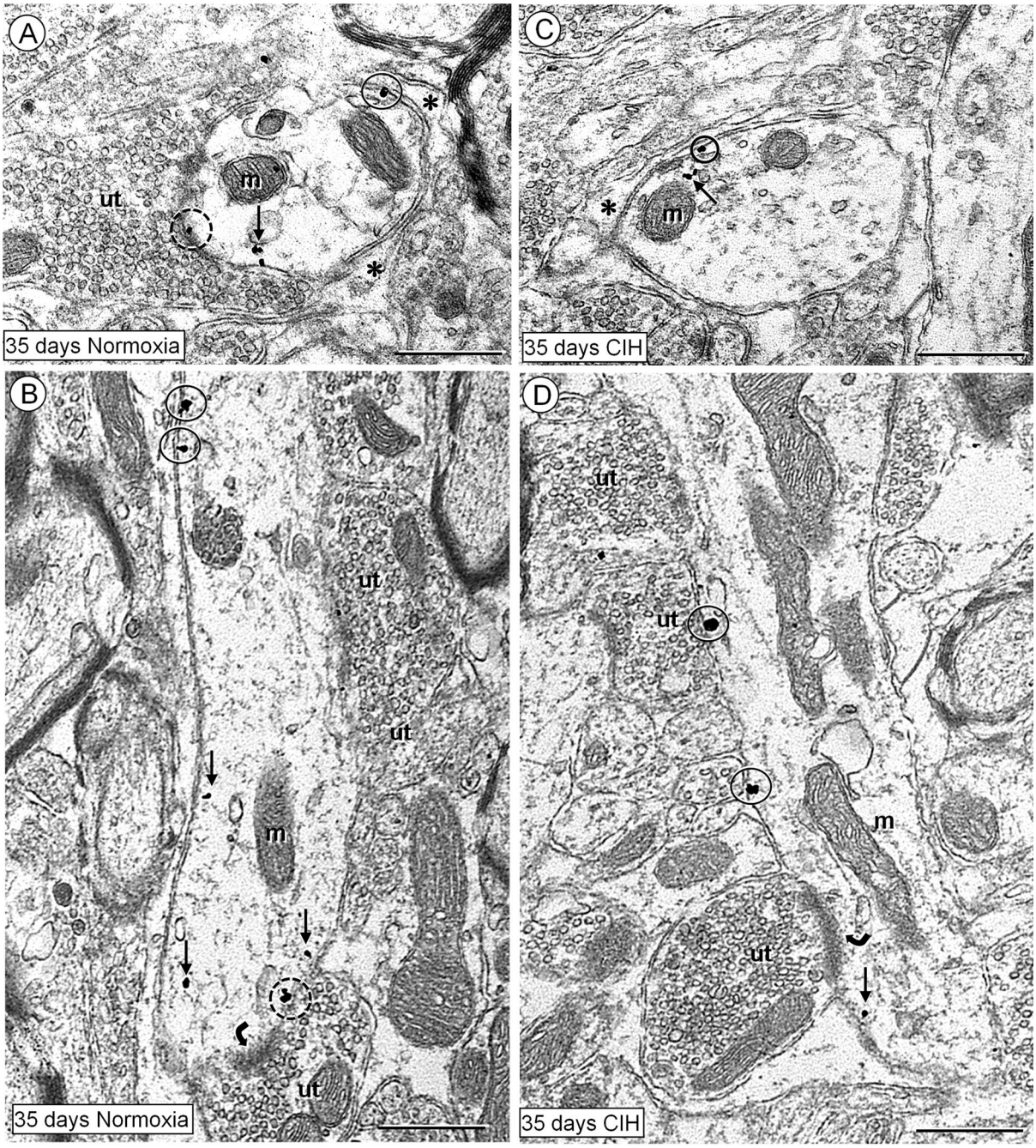

Fig. 6.

Electron micrographs displaying plasmalemmal (encircled) and cytoplasmic (arrows) distributions of NK_1 receptor immunogold particles in non-TH dendrites within the cNTS of mice receiving room air (normoxia) (A,B) or CIH (C,D) for 35 days. In the transverse (A) and longitudinal (B) sections of dendrites from controls, the NK_1 immunogold particles are seen in the cytosol (small arrows), and in contact with extrasynaptic (closed circles) or subsynaptic (dashed circles) plasma membrane. These dendrites receive symmetric (A) or asymmetric (curved arrow in B) synapses, and their non- synaptic surfaces are covered with glial processes (asterisk in A). Coronal (C) and longitudinal (D) sections of two dendrites in the cNTS of mice exposed to 35 days of CIH. In these dendrites, NK_1 immunogold particles are sparingly

distributed in the cytoplasm (arrows), and along non-synaptic portions of the plasma membrane. The dendrite in D receives an asymmetric synapse (curved arrow), from an unlabeled terminal (ut) and is opposed by several other unlabeled terminals (ut). Scale bars: 0.5 μm.

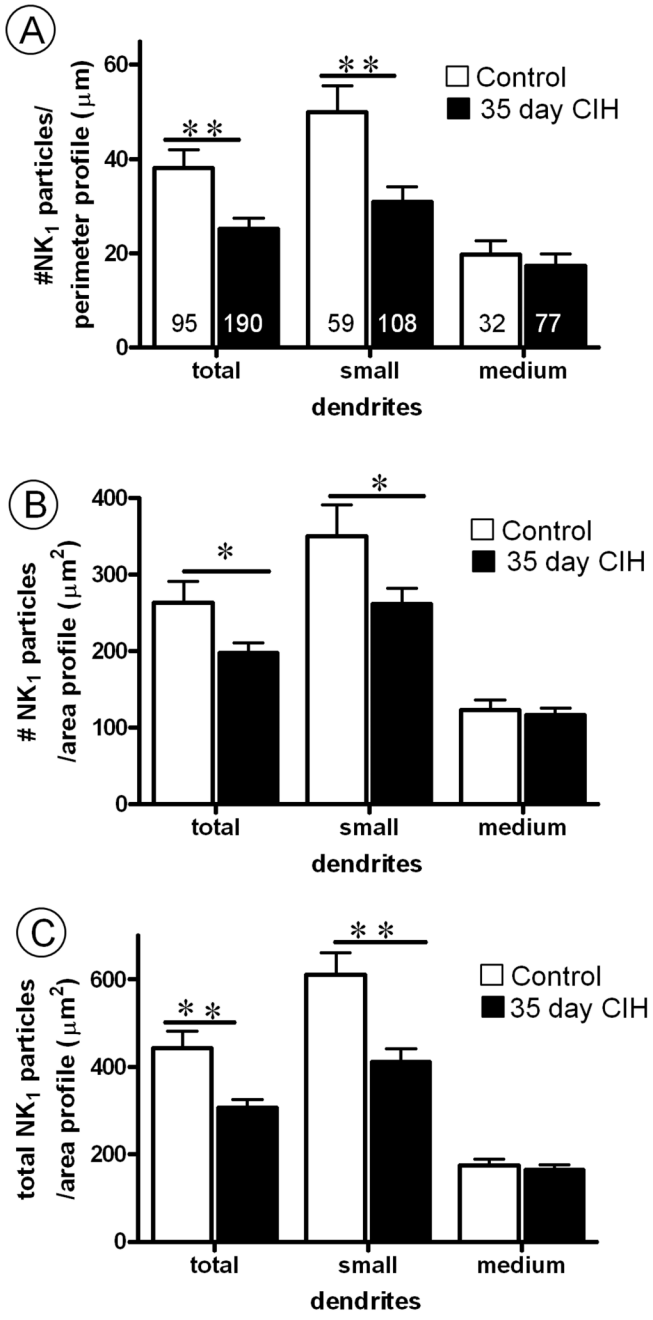

Fig. 7.

Bar graphs showing (A) plasmalemmal, (B) cytoplasmic and (C) total (plasmalemmal and cytoplasmic) NK_1 receptor density non-TH containing dendritic profiles in cNTS of control mice, as compared to mice subjected to 35 days of chronic intermittent hypoxia (CIH). In A, the values are given as ratio of the number of NK_1-immunogold particles contacting the dendritic plasma membrane/perimeter (100 μm. Numbers in bars represent the number of dendrites analyzed. In B, the values are given as the ratio of the number of NK_1 immunogold particles at a distance from the plasma membrane/area of the dendritic profile (100 μm^2). In C, the values are given as ratio of the total number of NK_1 immunogold particles/area of the dendritic profile (100 μm^2). Vertical bars represent the mean ± S.E. mean of (n) dendrites in

each group. Statistical comparisons were made between control and 35 days CIH mice in groups including all dendrites (total) or the subdivided categories of small (<1 μm) and medium-(1.1–2 μm) dendrites as indicated by their minimal cross-sectional diameter. Data were obtained from 8 vibratome sections, one for each of the four control and four 35 day CIH mice. Significant differences were determined using an unpaired Student *t*-test. **P< 0.01, *P< 0.05.

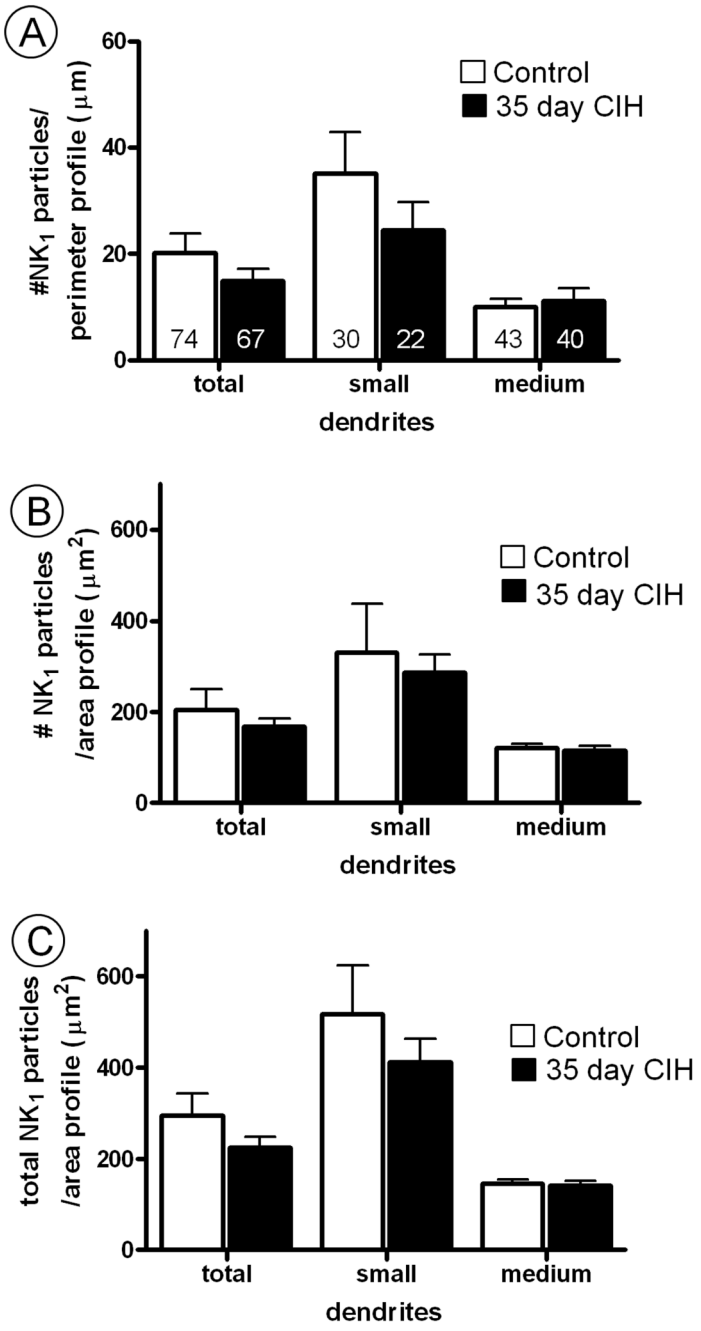

Fig. 8.

Quantitative assessment of the subcellular distribution of (A) plasmalemmal, (B) cytoplasmic and (C) total (plasmalemmal and cytoplasmic) NK_1 receptor density in dendritic profiles within the Sp-5 nucleus of control mice, as compared to mice subjected to 35 days of chronic intermittent hypoxia (CIH). In A, the ratio shown is the number of NK_1-immunogold particles contacting the plasma membrane/perimeter of the dendrite (100 μm). Numbers in bars represent the number of dendrites analyzed. In B, the ratio is given as number of NK_1 immunogold particles at a distance from the plasma membrane/area of the dendritic profile (100 μm^2). In C, the ratio is the total number of NK_1 immunogold particles/area of the dendritic profile (100 μm^2). Vertical bars represent the mean ± S.E. mean of (n) dendrites. Statistical

comparisons were made between control and 35 days CIH mice in groups including all transversely cut dendritic profiles (total) or the dendrites separated by minimal cross-sectional diameter into small (<1 μm) and medium (1.1–2 μm) sized categories. Data were obtained from 6 vibratome sections, one for each of the three control and three 35 day CIH mice analyzed. Unpaired Student *t*-test revealed no significant differences between control mice and those subjected to 35 days of CIH.

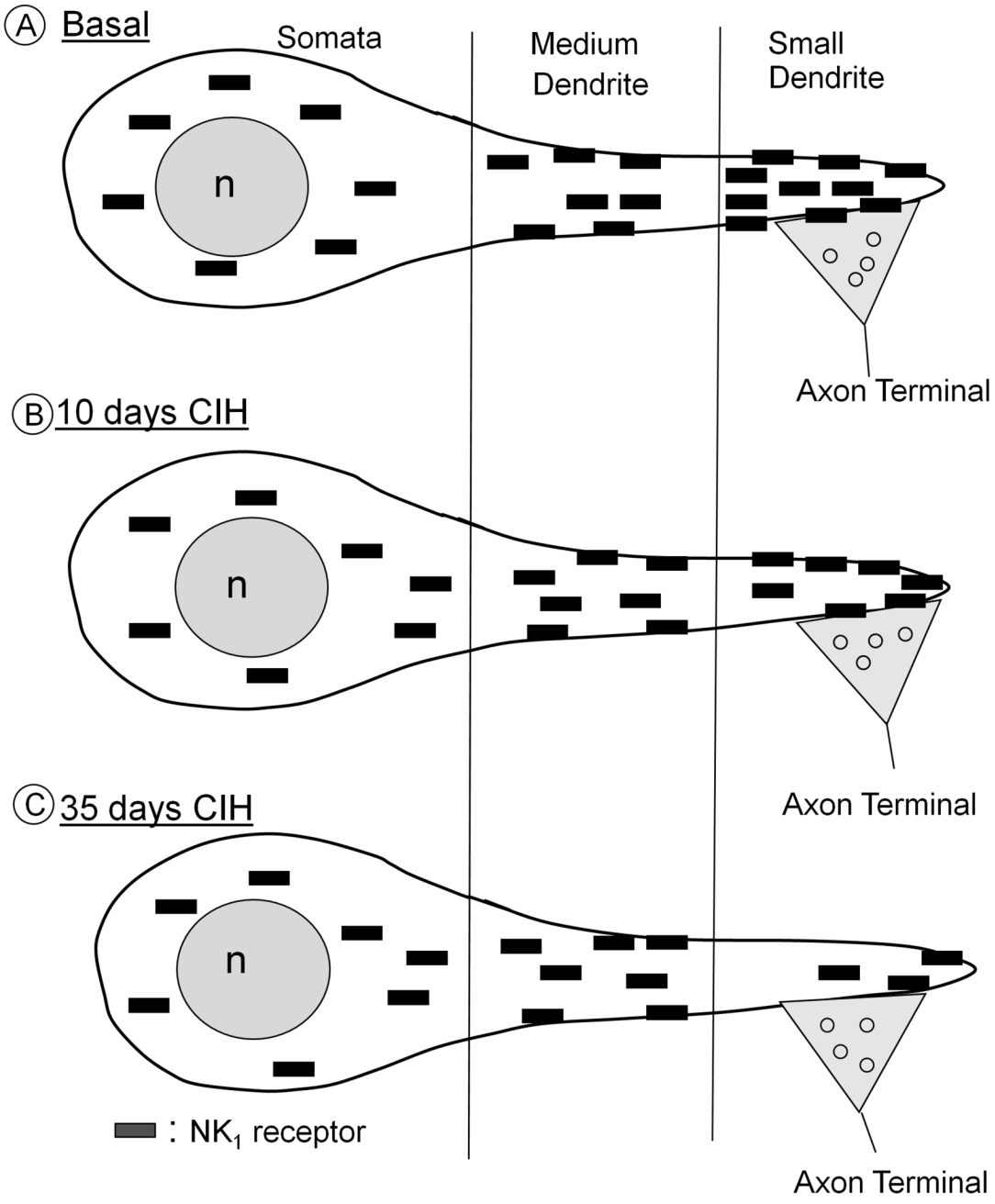

Fig. 9.

Simplified schematic representation of the basal (A) subcellular localization and 10 day (B) or 35 day (B) CIH-induced redistribution of NK_1 receptors (rectangles) in somatodendritic profiles of same-size neurons within the mouse cNTS. In all animals, these receptors are mainly seen in the cytoplasm (surrounding nucleus, n) of soma and in large proximal dendrites, but become increasingly prevalent on extrasynaptic (continuous outline) and synaptic (double dashed line beneath axon terminal) plasma membrane of smaller dendrites. A. Under resting conditions, the small dendrites show the greatest density of cytoplasmic as well as extrasynaptic plasmalemmal NK_1 receptors. B. Following 10 days of CIH, the cytoplasmic density of NK_1 receptors is decreased exclusively in smaller dendrites, which presumably receives

chemosensory inputs activated by hypoxic events. C. After 35 days of CIH, there is a significant decrease in both plasmalemmal and cytoplasmic NK_1 receptor density as compared with controls. For ease of presentation, the smaller dendrites are diagrammatically shown as distal portions of larger dendrites, but also may include small dendrites of small neurons that preferentially express NK_1 receptors, which are not shown in this schematic.

Table 1

Percentage of single NK_1-labeled profiles found in neuronal and glial compartments of the cNTS in control and CIH mice

Profile	Control	10 days CIH	35 days CIH
Neuronal Soma	8%	11%	6%
Dendrite	84%	81%	83%
Axon terminal	5%	5%	5%
Glial Process	3%	3%	4%
***Total**	446	241	333

*Number of profiles seen in one vibratome section through the cNTS of 7 sham control mice; three 10 day, and four 35 day CIH mice. The total areas of cNTS tissue include: 4,677 μm^2 in control; 3,779 μm^2 in 10 day, and 3,368 μm^2 in 35 day CIH mice.

Table 2

Subcellular compartmentation of NK_1 immunogold particles in non-TH containing dendrites in cNTS of control and CIH mice

Location	Control	10 days CIH	35 days CIH
Cytoplasm	63%	50%	67%
Extrasynaptic Plasmalemma	30%	41%	24%
Synaptic Plasmalemma	7%	9%	9%
***Total particles**	1,865	915	1,019

*Number of particles seen in one vibratome section through the cNTS of 7 sham control mice; three 10 day CIH, and four 35 day CIH mice. The total areas of cNTS tissue include: 4,677 μm^2 in control; 3,779 μm^2 in 10 day; and 3,368 μm^2 in 35 day CIH mice.